Progress In Electromagnetics Research C, Vol. 37, 53–66, 2013

A NEW DUAL BAND BALANCED-TO-BALANCED POWER DIVIDER

Bin Xia[1, 2, *] and Junfa Mao[2]

[1]Zhenjiang Watercraft College PLA, Zhenjiang City, Jiangsu 212003, China

[2]Key Lab of Ministry of Education for Research of Design and EMC of High Speed Electronic Systems, Shanghai Jiao Tong University, Shanghai 200240, China

Abstract—In this paper, a new dual band balanced-to-balanced power divider is proposed. By using the dual frequency 90° phase shifter based T model, the proposed balanced-to-balanced power divider can be deduced. By using the method in our previous work, the dual band balanced-to-balanced power divider could be designed with 1 : 1 power division. This balanced-to-balanced power divider is implemented on microstrip structure. Comparing the results calculated in analytical method with that simulated by the full-wave electromagnetic simulator, and that measured by the network analyzer, the final results show that they have a good mixed mode performance. The pass band 1 is from 2.395 GHz to 2.550 GHz, and the pass band 2 is from 5.245 GHz to 5.30 GHz. The maximum isolations for pass band 1 and pass band 2 are 17.8 dB and 17.6 dB, respectively.

1. INTRODUCTION

In modern communication system, multiple band application brought much more advantage [1, 2]. Semi-loop stepped-impedance resonators were used to design dual band power divider [3]. In designing dual-band Wilkinson power dividers, two section transmission lines with lumped elements [4–6], or open-ended stubs [7, 8] has been presented. Closed-form design method of N-way dual-band Wilkinson power dividers has been discussed in [9]. One section or two section

Received 17 December 2012, Accepted 10 January 2013, Scheduled 28 January 2013

* Corresponding author: Bin Xia (xiabinsjtu@163.com).

coupled line with one or two absorption resistors was studied in [10–15]. Periodically loaded slow wave structure was used for dual-band applications [16].

In [17], a three section transmission-line transformer with three isolation resistors was used to realize a triband power divider. In [18], dual- and tri-band equal split Wilkinson power dividers using composite right- and left-handed(CRLH) transmission lines (TLs) CRLH TLs with exact design equations were presented. In [19], the multiband power divider is constructed by attaching the transformer to each port of the junction.

The balanced circuit has attracted much attention for its higher immunity to environmental noise than the unbalanced circuits. In our previous work [20], a new balanced-to-balanced power divider was firstly proposed to design all-balanced RF frontend. However, the design only focused on single band application.

In this paper, a new dual band balanced-to-balanced power divider is proposed. By using matrix transformation, the dual frequency phase shifter with 90° phase difference for the proposed balanced-to-balanced power divider can be deduced. By using the method proposed in [20], the dual band balanced-to-balanced power divider could be designed with 1 : 1 power division in a pure planar structure. A balanced-to-balanced power divider is implemented on microstrip structure with frequencies locating at 2.4 GHz and 5.2 GHz. Comparing the results calculated in analytical method with that simulated by the full-wave electromagnetic simulator, and that measured by the network analyzer, the final results show that they have a good mixed mode performance.

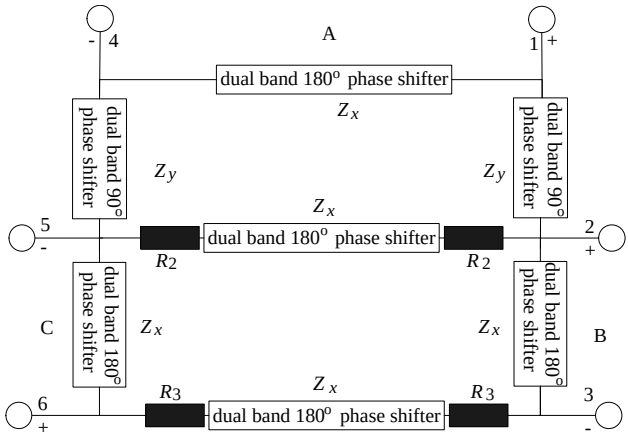

Figure 1. The proposed dual band balanced-to-balanced power divider.

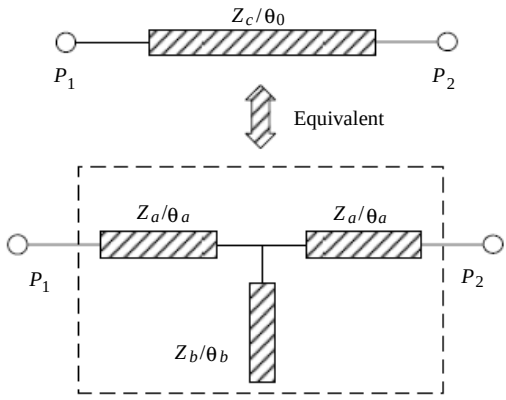

Figure 2. Dual band 90° phase shifter with T model.

Furthermore, the proposed balanced-to-balanced power divider is fabricated and measured to verify this concept. Its performance of mixed-mode power division and isolation will be shown in this work.

2. THE DUAL FREQUENCY PHASE SHIFTER WITH 90° PHASE DIFFERENCE

2.1. Dual Band 90° Phase Shifter Based on the *T* model

As Shown in Figure 2, T model is usually to replace the quarter-wavelength transmission line [21]. The S parameter of T model can be computed by multiplying the cascading $ABCD$ matrixes,

$$\begin{bmatrix} A_T(\theta) & B_T(\theta) \\ C_T(\theta) & D_T(\theta) \end{bmatrix} = \begin{bmatrix} \cos(\theta_a) & jZ_a \sin(\theta_a) \\ \frac{j\sin(\theta_a)}{Z_a} & \cos(\theta_a) \end{bmatrix} \begin{bmatrix} 1 & 0 \\ jY_b \tan(\theta_b) & 1 \end{bmatrix} \begin{bmatrix} \cos(\theta_a) & jZ_a \sin(\theta_a) \\ \frac{j\sin(\theta_a)}{Z_a} & \cos(\theta_a) \end{bmatrix} \quad (1)$$

$$A_T(\theta) = [\cos(\theta_a) - Z_a \sin(\theta_a) Y_b \tan(\theta_b)] \cos(\theta_a) - \sin^2(\theta_a) \quad (2a)$$

$$B_T(\theta) = jZ_a \sin(\theta_a) [\cos(\theta_a) - Z_a \sin(\theta_a) Y_b \tan(\theta_b)] + jZ_a \sin(\theta_a) \cos(\theta_a) \quad (2b)$$

$$C_T(\theta) = j\left[\frac{\sin(\theta_a)}{Z_a} + \cos(\theta_a) Y_b \tan(\theta_b)\right] \cos(\theta_a) + \frac{j\sin(\theta_a)}{Z_a} \cos(\theta_a) \quad (2c)$$

$$D_T(\theta) = -\left[\frac{\sin(\theta_a)}{Z_a} + \cos(\theta_a) Y_b \tan(\theta_b)\right] Z_a \sin(\theta_a) + \cos^2(\theta_a) \quad (2d)$$

The $ABCD$ matrix of the quarter-wavelength transmission line can be rewritten as

$$\begin{bmatrix} A_Q(\theta_0) & B_Q(\theta_0) \\ C_Q(\theta_0) & D_Q(\theta_0) \end{bmatrix} = \begin{bmatrix} \cos(\theta_0) & jZ_c\sin(\theta_0) \\ \frac{j\sin(\theta_0)}{Z_c} & \cos(\theta_0) \end{bmatrix} \tag{3}$$

$$\theta_0 = \frac{\pi}{2}, \ldots \tag{4}$$

The odd times quarter-wavelength transmission lines have similar characters, and all of them can be used to transfer impedance, and provide 90° phase difference. For dual band application, if the frequency ratio is n and n means the times of the center frequency of the second passband comparing with the center frequency of the first passband, the following condition is required;

$$A_T(\theta) = A_Q(\theta_0) \tag{5a}$$

$$A_T(n\theta) = A_Q(m\theta_0) \tag{5b}$$

$$B_T(\theta) = B_Q(\theta_0) \tag{5c}$$

$$B_T(n\theta) = B_Q(m\theta_0) \tag{5d}$$

$$C_T(\theta) = C_Q(\theta_0) \tag{5e}$$

$$C_T(n\theta) = C_Q(m\theta_0) \tag{5f}$$

$$D_T(\theta) = D_Q(\theta_0) \tag{5g}$$

$$D_T(n\theta) = D_Q(m\theta_0) \tag{5h}$$

It must be mentioned that m is an odd positive integer, and n is a rational number. Using Equations (5a), (5c), (5e), (5g) and (2a)–(2d), the following results can be obtained,

$$\tan(\theta_a) = \frac{Z_c}{Z_a} \tag{6a}$$

$$\tan(\theta_b) = \frac{2Z_b}{Z_a\tan 2(\theta_a)} = \frac{Z_b(Z_a^2 - Z_c^2)}{Z_a^2 Z_c} \tag{6b}$$

Similar results are shown in Equations (5a), (5c) all presented in [4] for single band application. Using Equations (5b), (5d), (5f), (5h), following results can be obtained,

$$\tan(n\theta_a) = \frac{Z_c}{Z_a}\sin(m\theta_0) \tag{7a}$$

$$\tan(n\theta_b) = \frac{2Z_b}{Z_a\tan(2n\theta_a)} = \frac{Z_b(Z_a^2 - Z_c^2)}{Z_a^2 Z_c\sin(m\theta_0)} \tag{7b}$$

2.2. Discussion for Different n and m

Though the values of m odd positive integer can be determined in wide range, $\sin m\theta_0$ have only two values: $\sin m\theta_0 = 1$ for $m = 4t + 1$;

Table 1. The electronic parameters at intersection point for $N = 2$.

	P_1	P_2	P_3	P_4
	Θ_a	Θ_b	Θ_a	Θ_b
degree	60	120	240	300
$\tan\theta$	1.732	-1.732	1.732	-1.732
$-\tan 2\theta$	1.732	-1.732	1.732	-1.732
Z_a/Z_c	0.577	-	0.577	-
Z_b/Z_c	-	0.866	-	0.866

$\sin m\theta_0 = -1$ for $m = 4t + 3$, where t is integer and $t \geq 0$. To simplify the problem, we consider only $m = 1$ and 3, that is enough for the dual band application. In the following discussion, $0 < \theta_a < 2\pi$, $0 < \theta_b < 2\pi$.

Case of $m = 1$:

From (6a)–(6b), (7a)–(7b), we have

$$\tan(n\theta_a) = \tan(\theta_a) = \frac{Z_c}{Z_a} \tag{8a}$$

$$\tan(n\theta_b) = \tan(\theta_b) = \frac{Z_b(Z_a^2 - Z_c^2)}{Z_a^2 Z_c} \tag{8b}$$

Case of $m = 3$:

We have

$$\tan(\theta_a) = \frac{Z_c}{Z_a} \tag{9a}$$

$$\tan(n\theta_a) = -\frac{Z_c}{Z_a} \tag{9b}$$

$$\tan(\theta_b) = \frac{Z_b\left(Z_a^2 - Z_c^2\right)}{Z_a^2 Z_c} \tag{9c}$$

$$\tan(n\theta_b) = -\frac{Z_b\left(Z_a^2 - Z_c^2\right)}{Z_a^2 Z_c} \tag{9d}$$

From Table 1, we can find that the points of P_1 and P_2 are a group of solutions of T model for dual frequency phase shifter with 90° phase difference, and P_3 and P_4 are another group of solutions of T model for dual frequency phase shifter with 90° phase difference in the electrical length range of $0 < \theta_a < 2\pi$, $0 < \theta_b < 2\pi$. Comparing the two groups of solutions, P_1 and P_2 are better choice for their compact sizes.

Table 2. The electronic parameters at intersection point for $N = 3$.

	P_1	P_2	P_3	P_4
	Θ_a	Θ_b	Θ_a	Θ_b
degree	45	0	235	0
$\tan\theta$	1	0	1	0
$-\tan 3\theta$	1	0	1	0
Z_a/Z_c	1	-	1	-
Z_b/Z_c	-	-	-	-

Table 3. The electronic parameters at intersection point for $N = 4$.

	P_1	P_1	P_2	P_3	P_4	P_4	P_5	P_6
	Θ_a	Θ_b	Θ_a	Θ_b	Θ_a	Θ_b	Θ_a	Θ_b
degree	36	36	72	108	216	216	252	288
$\tan\theta$	0.73	0.73	3.08	-3.08	0.73	0.73	3.08	-3.08
$-\tan 4\theta$	0.73	0.73	3.08	-3.08	0.73	0.73	3.08	-3.08
Z_a/Z_c	1.38	-	0.32	-	1.38	-	0.32	-
Z_b/Z_c	-	1.54	-	0.36	-	1.54	-	0.36

From Table 2, we can find that the points of P_1 and P_3 are two solutions of T model for 90° dual frequency phase shifter, and $P_2 = P_4 = 0$ means that T-model can be as transmission line without stub loaded.

From Table 3, we can find that the points of P_1 is the first solution of T model for dual frequency phase shifter with 90° phase difference, P_2 and P_3 the second solution, P_4 the third solution, and P_5 and P_6 the forth solution in the electrical length range of $0 < \theta_a < 2\pi$, $0 < \theta_b < 2\pi$. Selecting the first solution, the size of dual frequency phase shifter with 90° phase difference is compact.

2.3. Dual Band 180° Phase Shifter

Cascading two dual band 90° phase shifter, we can get 180° dual band phase shifter. So, to simplify the design process, we use the two dual band 90° phase shifter with T model to realize the 180° dual band phase shifter.

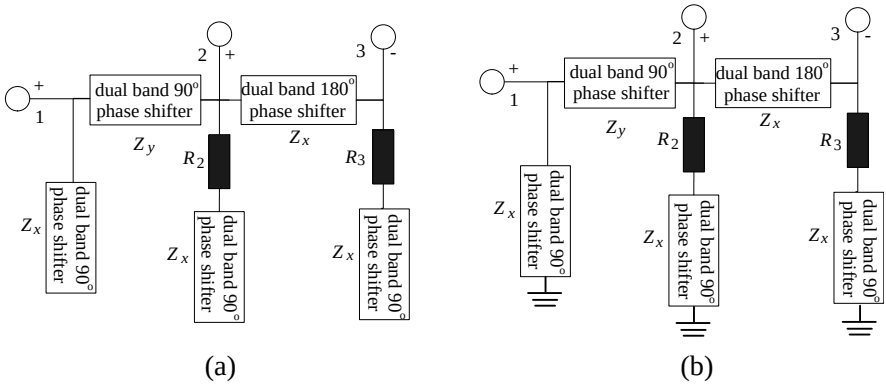

Figure 3. (a) Even-mode and (b) odd-mode circuit model of the proposed dual band balanced-to-balanced power divider/combiner.

3. DUAL BAND BALANCED-TO-BALANCED POWER DIVIDER

3.1. The Whole Equivalent Circuit Model of Balanced-to-balanced Power Divider with Ideal Device Model

As shown in Figure 3, it is easy to obtain the even-mode circuit model from Figure 1, which is a three-port network with each port matched to $Z = 50\,\Omega$. Obviously, if we set $Z_y = 35.355\,\Omega$.

$$\frac{1}{R_2} + \frac{1}{R_3} = \frac{2}{Z_0} \tag{10a}$$

$$Z_y = \frac{\sqrt{2}Z_0}{2} \tag{10b}$$

According to (10), the three-port scattering matrices of the even- and odd-mode circuit models at the central frequencies f_{01} and f_2 of the proposed dual band balanced-to-balanced power divider/combiner are all derived as

$$[S_e] = \begin{bmatrix} -1 & 0 & 0 \\ 0 & -\frac{1}{2} & -\frac{1}{2} \\ 0 & -\frac{1}{2} & -\frac{1}{2} \end{bmatrix} \tag{11a}$$

$$[S_o] = \begin{bmatrix} 0 & -j\frac{\sqrt{2}}{2} & j\frac{\sqrt{2}}{2} \\ -j\frac{\sqrt{2}}{2} & -\frac{1}{2} & -\frac{1}{2} \\ j\frac{\sqrt{2}}{2} & -\frac{1}{2} & -\frac{1}{2} \end{bmatrix} \tag{11b}$$

Obviously, (11a) and (11b) satisfy the constraint rule of odd- and even-mode scattering matrices of the balanced-to-balanced power divider/combiner that was proposed in the works [20]. Using the matrix transformation in [20], the mixed mode scattering matrix can be derived as,

$$[S^{mm}] = \begin{bmatrix} 0 & j\frac{\sqrt{2}}{2} & j\frac{\sqrt{2}}{2} & 0 & 0 & 0 \\ j\frac{\sqrt{2}}{2} & 0 & 0 & 0 & 0 & 0 \\ j\frac{\sqrt{2}}{2} & 0 & 0 & 0 & 0 & 0 \\ 0 & 0 & 0 & -1 & 0 & 0 \\ 0 & 0 & 0 & 0 & -1 & 0 \\ 0 & 0 & 0 & 0 & 0 & -1 \end{bmatrix} \tag{12}$$

3.2. Dual Band Balanced-to-balanced Power Divider for WLAN (2.45/5.2 GHz)

The operating frequencies of the proposed dual band balanced-to-balanced power divider are designed for the applications of the modern WLAN (2.45/5.2 GHz) systems, where $n = 2.12$. So, we have,

$$\theta_a = \frac{\pi}{n+1} \tag{13a}$$

$$Z_a = \frac{Z_c}{\tan(\theta_a)} \tag{13b}$$

$$\theta_b = \frac{2\pi}{n+1} \tag{13c}$$

$$Z_b = \frac{Z_a^2 Z_c \tan(\theta_b)}{(Z_a^2 - Z_c^2)} \tag{13d}$$

Based on (13), a prototype of the dual-band balanced-to-balanced power divider/combiner is designed with the central frequency of $f_{01} = 2.45\,\text{GHz}$ and $f_{02} = 5.2\,\text{GHz}$. We set $Z_x = 50\,\Omega$. The theoretical results are shown in Figure 3, where the lossless transmission lines and ideal lumped resistors are used. Since the balanced ports B and C are symmetric, some mixed-mode S-parameters are omitted. Note that the S-parameters are identified as $S_{dd\text{AB}}$, which refers to the differential to differential mode between ports B and A in Figure 1, and the other S-parameters use a similar naming system. Note that the value of $S_{cdAA} = S_{dcAA}$ is always equal to zero due to the symmetry between ports 1 and 4, and the corresponding theoretical curves are not plotted in Figure 4(b).

As shown in Figure 4, the differential-mode transmission coefficient and common-mode reflection coefficient reach their

maximum of $|S_{dd\mathrm{AB}}| = -3.01\,\mathrm{dB}$ and $|S_{cc\mathrm{AA}}| = |S_{cc\mathrm{BB}}| = 0\,\mathrm{dB}$ at $f_{01} = 2.45\,\mathrm{GHz}$ and $f_{02} = 5.2\,\mathrm{GHz}$, respectively. All the other mixed-mode S-parameters approach zero at f_0.

If the value of $|S_{dd\mathrm{AB}}|$ better than $-4\,\mathrm{dB}$ and the values of $|S_{dd\mathrm{AA}}|$, $|S_{dd\mathrm{BB}}|$, $|S_{dd\mathrm{BC}}|$, $|S_{cc\mathrm{AB}}|$, $|S_{cc\mathrm{BC}}|$, $|S_{cd\mathrm{BB}}|$, $|S_{cd\mathrm{AB}}|$, $|S_{cd\mathrm{BC}}|$, $|S_{dc\mathrm{BB}}|$, $|S_{dc\mathrm{AB}}|$, $|S_{dc\mathrm{BC}}|$ all better than $-15\,\mathrm{dB}$ should be satisfied simultaneously, an operating band can be achieved within 2.375 to 2.60 GHz, and 5.035 to 5.27 GHz, i.e., the bandwidth of about 22.5 MHz. It can be seen that the dual pass bands have equal bandwidths, too.

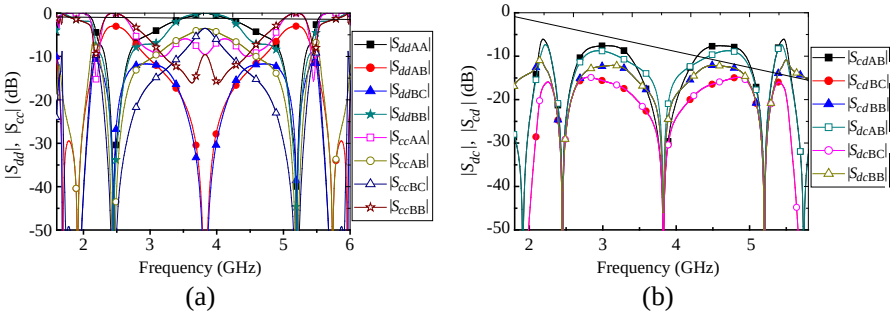

Figure 4. The theoretical mixed-mode S-parameters of the dualband balanced-to-balanced power divider/combiner prototype with central frequency located at 2.45 GHz and 5.2 GHz, respectively: (a) S_{dd} and S_{cc}; (b) S_{cd} and S_{dc}.

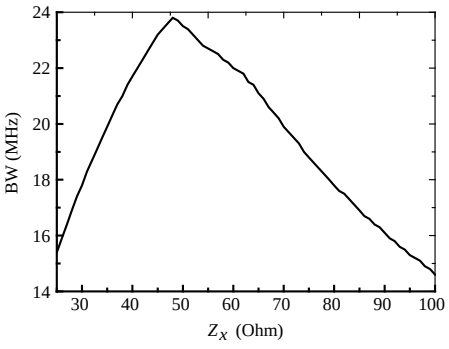

Figure 5. The bandwidth of the dual band balanced-to-balanced power divider/combiner with variable Z_x.

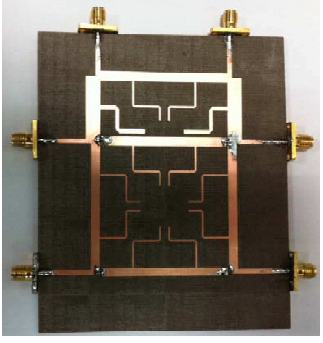

Figure 6. Photo of the balanced-to-balanced power divider/combiner prototype.

The influence of characteristic impedance Z_x on bandwidths of the dual band is further studied numerically by using the method proposed in [15]. From Figure 5, we can find that the proposed power divider has its maximum bandwidth of 23.8 MHz with $Z_x = 48\,\Omega$.

4. RESULTS AND DISCUSSION

As shown in Figure 6, the prototype is realized with microstrip lines and surface-mounted lumped resistors and fabricated on a F4B substrate with the relative permittivity of $\varepsilon_r = 2.65$, the loss tangent of $\tan\delta = 0.003$ and the thicknesses of $h = 0.73$ mm.

Its critical design parameters are $Z_{a1} = 22.40\,\Omega$, $Z_{b1} = 50.14\,\Omega$, $\theta_{a1} = \theta_{a2} = 57.65°$, $\theta_{b1} = \theta_{b2} = 115.30°$, $Z_{a2} = 32.41\,\Omega$, $Z_{b2} = 62.09\,\Omega$, where "1" denotes the designed "T" dual band shifter with equivalent impedance $Z_y = 35.35\,\Omega$, and "2" denotes the designed "T" dual band shifter with equivalent impedance $Z_x = 48\,\Omega$.

The six-port S-parameters are simulated by the commercial software, Ansoft HFSS, and measured with the four-port vector network analyzer, Agilent E5071.

Figures 7(a) and (b) show a comparison between the simulated and measured transmission coefficients, reflection coefficients and isolation between the balanced ports B and C for differential- and common-mode operation, respectively. Figures 7(c) and (d) provide a comparison between the simulated and measured differential-to-common and common-to-differential mode conversions. Figure 10(e) shows the magnified curves of $|S_{dd\mathrm{AB}}|$, $|S_{cc\mathrm{AA}}|$ and $|S_{cc\mathrm{BB}}|$.

In the measurements, the maximum differential-mode transmission coefficient of the prototype is $|S_{dd\mathrm{AB}}| = -3.92$ dB at 2.47 GHz, $|S_{dd\mathrm{AB}}| = -4.76$ dB at 5.3 GHz, and the common-mode reflection coefficients of $|S_{cc\mathrm{AA}}|$ and $|S_{cc\mathrm{BB}}|$ reach their maximum of -0.29 and -0.84 dB at 2.51 and 2.50 GHz, and the common-mode reflection coefficients of $|S_{cc\mathrm{AA}}|$ and $|S_{cc\mathrm{BB}}|$ reach their maximum of -0.54 and -1.43 dB at 5.38 and 5.36 GHz for band 2, respectively. The pass

Table 4. Performance comparison with previous works.

	Isolation (dB)	Fractional bandwidth (%)	band	center frequency (GHz)
Ref. [20]	47.2	20.8	1	2
Ref. [22]	-	13.0	1	5.2
this work	17.8/17.6	6.5/4.9	2	2.4/5.2

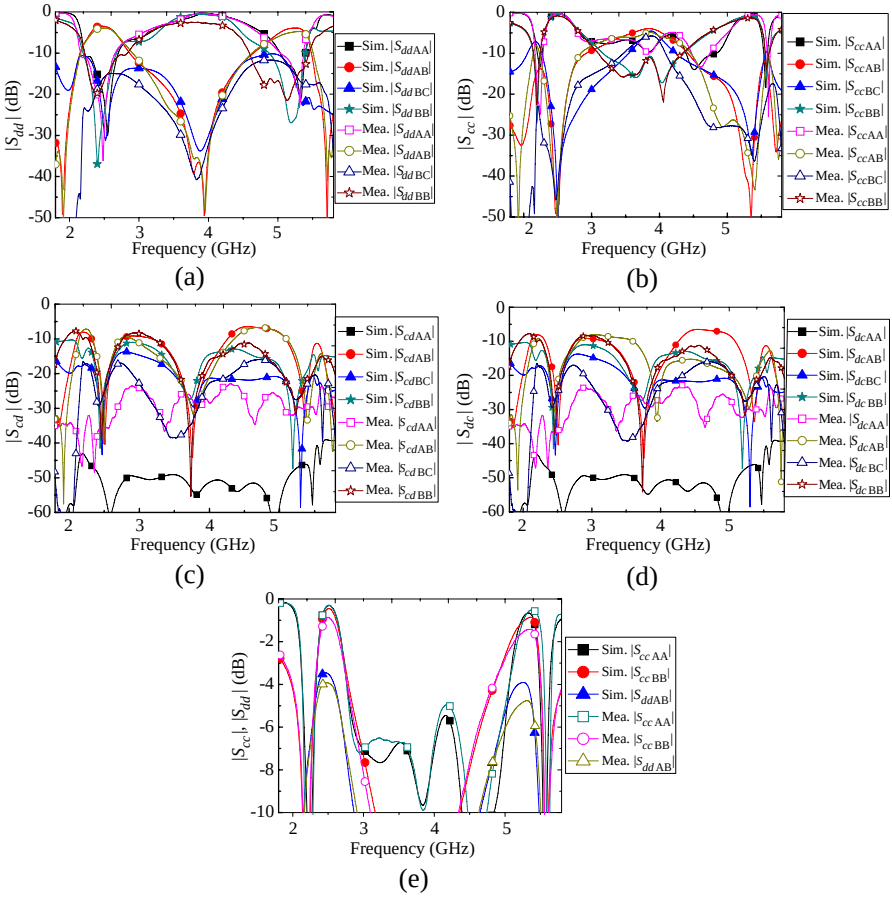

Figure 7. The simulated and measured mixed-mode S-parameters of the dual band balanced-to-balanced power divider with the center frequency of the two passband at 2.45 GHz and 5.25 GHz respectively, (a) $|S_{dd}|$; (b) $|S_{cc}|$; (c) $|S_{cd}|$; (d) $|S_{dc}|$; and (e) the magnified curves of $|S_{dd\mathrm{AB}}|$, $|S_{cc\mathrm{AA}}|$ and $|S_{cc\mathrm{BB}}|$. Mea.: Measured results. Sim.: Simulated results.

band 1 is from 2.395 GHz to 2.550 GHz and pass band 2 from 5.245 GHz to 5.30 GHz. The maximum isolations for pass band 1 and pass band 2 are 17.8 dB and 17.6 dB, respectively. The difference between the simulated and measured results is mainly caused by the non-ideal symmetry of the fabricated prototype which is also due to the tolerance of fabrication, coupling effects between the parts of the transmission lines which affect equivalent electronic parameters of the stub, and non-

ideal surface-mounted resistors. This symmetric layout solution may have least coupling effect. The performance comparisons with previous works is given in Table 4. Dual-band balanced-to-balanced power divider has smaller fractional bandwidth than the one-band application.

5. CONCLUSION

In this paper, a new concept of dual band balanced-to-balanced power divider/combiner is proposed, which can realize dual band power division in a balanced RF front-end. Firstly, a dual band 90° shifter based T model for a different frequency ratio is analyzed by matrix transformation. Then, our proposed dual band balanced-to-balanced power divider/combiner is built up with a combination of ideal shifter and resistances. Further, a prototype is realized by microstrip lines and surface-mounted lumped resistors to demonstrate our design. Good agreement has been obtained between the simulated and measured mixed-mode S-parameters. It is found that an equal power division and combining between two balanced ports is achieved only with the proposed component, which leads to simplified system architecture and low loss. Though the size is some bulky miniaturization technology can be used to deduce the size in future study. It can be expected that the new dual band balanced-to-balanced power divider/combiner will be valuable in the further fully-balanced RF front-ends.

ACKNOWLEDGMENT

This work was supported in part by the National Basic Research Program of China under Grant of 2009CB320204.

REFERENCES

1. Perumana, B. G., J.-H. C. Zhan, S. S. Taylor, B. R. Carlton, and J. Laskar, "Resistive-feedback CMOS low-noise amplifiers for multiband applications," *IEEE Trans. Microw. Theory Tech.*, Vol. 56, No. 5, 1218–1225, May 2008.
2. Kuo, Y.-T., J.-C. Lu, C.-K. Liao, and C.-Y. Chang, "New multiband coupling matrix synthesis technique and its microstrip implementation," *IEEE Trans. Microw. Theory Tech.*, Vol. 58, No. 7, 1840–1850, Jul. 2010.
3. Avrillon, S., I. Pele, A. Chousseaud, and S. Toutain, "Dual-band power divider based on semiloop stepped-impedance resonators,"

IEEE Trans. Microw. Theory Tech., Vol. 51, No. 4, 1269–1273, Apr. 2003.

4. Wu, L., Z. Sun, H. Yilmaz, and M. Berroth, "A dual-frequency Wilkinson power divider," *IEEE Trans. Microw. Theory Tech.*, Vol. 54, No. 1, 278–284, Jan. 2006.
5. Park, M.-J. and B. Lee, "A dual-band Wilkinson power divider," *IEEE Microw. Wireless Compon. Lett.*, Vol. 18, No. 2, 85–87, Feb. 2008.
6. Wu, Y., Y. Liu, and S. Li, "Dualband modified Wilkinson power divider without transmission line stubs and reactive components," *Progress In Electromagnetics Research*, Vol. 96, 9–20, 2009.
7. Cheng, K.-K. M. and F.-L. Wong, "A new Wilkinson power divider design for dual band application," *IEEE Microw. Wireless Compon. Lett.*, Vol. 17, No. 9, 664–666, Sep. 2007.
8. Shin, Y., B. Lee, and M.-J. Park, "Dual-band Wilkinson power dividerwith shifted output ports," *IEEE Microw. Wireless Compon. Lett.*, Vol. 18, No. 7, 443–445, Jul. 2008.
9. Wu, Y. L., Y. A. Liu, S. L. Li, C. P. Yu, and X. Liu, "Closed-form design method of an N-way dualband Wilkinson hybrid power dividers," *Progress In Electromagnetics Research*, Vol. 101, 97–114, 2010
10. Park, M.-J., "Two-section cascaded coupled line Wilkinson power divider for dual-band applications," *IEEE Microw. Wireless Compon. Lett.*, Vol. 57, No. 4, 188–190, Apr. 2009.
11. Park, M.-J., "Dual-band Wilkinson divider with coupled output port extensions," *IEEE Trans. Microw. Theory Tech.*, Vol. 57, No. 9, 2232–2237, Sep. 2009.
12. Lin, Z. and Q.-X. Chu, "A novel approach to the design of dualband Wilkinson power divider with variable power dividing ratio based on coupled-lines," *Progress In Electromagnetics Research*, Vol. 96, 9–20, 2010.
13. Wu, Y., Y. Liu, and Q. Xue, "An analytical approach for a novel coupled-line dual-band Wilkinson power divider," *IEEE Trans. Microw. Theory Tech.*, Vol. 59, No. 2, 286–294, Feb. 2011.
14. Li, B., "Dualband equal/unequal Wilkinson power dividers based on coupling section with short-circuited stub," *Progress In Electromagnetics Research*, Vol. 111, 163–178, 2011.
15. Li, J. C., Y. L. Wu, Y. A. Liu, J. Y. Shen, S. L. Li, and C. P. Yu, "A generalized coupledline dualband Wilkinson power divider with extended ports," *Progress In Electromagnetics Research*, Vol. 129, 197–214, 2012.

16. Rawat, K. and F. M. Ghannouchi, "A design methodology for miniaturized power dividers using periodically loaded slow wave structure with dual-band applications," *IEEE Trans. Microw. Theory Tech.*, Vol. 57, No. 12, 3280–3288, Dec. 2009.
17. Chongcheawchamnan, M., S. Patisang, M. Krairiksh, and I. Robertson,"Tri-band Wilkinson power divider using a three-section transmission-line transformer," *IEEE Microw. Wireless Compon. Lett.*, Vol. 16, No. 8, 452–454, Aug. 2006.
18. Genc, A. and R. Baktur,, "Dual- and triple-band Wilkinson power dividers based on composite right- and left-handed transmission lines," *IEEE Trans. Microw. Theory Tech.*, Vol. 54, No. 1, 327–334, Mar. 2011.
19. Chu, Q.-X., F. Lin, Z. Lin, and Z. Gong, "Novel design method of tri-band power divider," *IEEE Trans. Microw. Theory Tech.*, Vol. 54, No. 1, 2221–2226, Nov. 2011.
20. Xia, B., L.-S. Wu, and J. Mao, "A new balanced-to-balanced power divider/combiner," *IEEE Trans. Microw. Theory Tech.*, Vol. 60, No. 9, 287–295, Sep. 2012.
21. Wu, Y., Y. Liu, Y. Zhang, J. Gao, H. Zhou and Q. Xue, "A dual band unequal Wilkinson power divider without reactive components," *IEEE Trans. Microw. Theory Tech.*, Vol. 57, No. 1, 216–222, Jan. 2009.
22. Wu, L.-S., B. Xia, and J. Mao, "A new balanced-to-balanced power divider/combiner," *IEEE Microw. Wireless Compon. Lett.*, Vol. 20, No. 1, 19–21, Jan. 2012.